Supporting Information

Performance and mechanism of Carbamazepine removal in the FeS-$S_2O_8^{2-}$ process: experimental investigation and DFT calculations

Xuejun Long[a,b], Jun Luo[a], Zhenxing Zhong[a,b,*], Yanxu Zhu[c], Chunjie Zhang[c], Jun Wan[a,b], Haiyan Zhou[d], Beiping Zhang[e], Dongsheng Xia [a,b]

[a] *College of Environmental Engineering, Wuhan Textile University, Wuhan 430200, China*

[b] *Engineering Research Center for Clean Production of Textile Printing and Dyeing, Ministry of Education, Wuhan Textile University, Wuhan 430073, China*

[c] *Central & Southern China Municipal Engineering Design and Research Institute Co, Ltd, Wuhan, 430010, China*

[d] *Soil Environmental Institute, Guangdong Provincial Academy of Environmental Science, Guangzhou 510045, China*

[e] *School of Environmental Science and Engineering, Huazhong University of Science and Technology, Wuhan 430074, China*

**Corresponding authors: xing2006z@163.com;*

A. Supplementary Texts

B. Supplementary Tables

C. Supplementary Figures

D. References

A. Supplementary Texts

Text S1. Chemicals

Sodium chloride (NaCl), sodium bicarbonate ($NaHCO_3$), dipotassium hydrogen phosphate (K_2HPO_4), tert-butyl alcohol (TBA), and ethyl alcohol (EtOH) were obtained from Sinopharm Chemical Reagent (Shanghai, China). 5,5-dimethyl-1-pyrolin-N-oxide (DMPO) was obtained from Aladdin Chemistry Co. (Shanghai, China). Methanol and acetonitrile (HPLC grade) were purchased from J&T Baker Chemical (USA). Other reagents and solvents were all in analytical grade or better.

Text S2. Testing methods of Fe^{2+}, total iron (TFe), $S_2O_8^{2-}$, and reactive radicals

The contents of Fe^{2+} and total iron (TFe) in aqueous were exactly quantified by employing an UV–vis spectrophotometer (UV-2600, Shimadzu, Kyoto, Japan), according to the 1,10-phenanthroline method [1]. Iodometric titration method was employed to detect persulfate ($S_2O_8^{2-}$) [2].

To explore the degradation mechanisms of CBZ in the FeS-$S_2O_8^{2-}$ process, the involved radicals were characterized by the radical quenching and Electron Paramagnetic Resonance (EPR) tests. During the scavenging experiments, two scavengers (150 mmol/L), tert-butyl alcohol (TBA, an $^{\bullet}OH$ scavenger) and ethyl alcohol (EtOH, a scavenger for both $^{\bullet}OH$ and $SO_4^{\bullet-}$), were added into the reaction solution, respectively. To detect the generation of $^{\bullet}OH$ and $SO_4^{\bullet-}$ directly during the reaction, ESR tests were carried out on a Bruker MEX-nano spectrometer using DMPO as the radical spin-trapping reagent, the modulation frequency was 100 kHz and the microwave power was 15 mW.

Text S3. Products identification and material characterization methods

The degradation products of CBZ in the FeS-$S_2O_8^{2-}$ process were detected by using a HPLC-APCI-MS (Agilent 1200, USA), equipped with an Agilent-C18 column (2.1 × 100 mm, 5μm) and a diode array detector. The column was maintained at 30 ^oC during analysis. The measurements were performed in a gradient elution program with methanol and water (0.1 % formic acid) as mobile phase. During 0-5 min, the proportion of methanol and water (0.1 % formic acid) were 60:40, and the proportion was 20:80 during 5-15 min. Flow rate was kept at 0.2 mL/min, the detection wavelengths were set at 211, 286, and 254 nm, the injection volume was 20 μL.

The primary elemental contents and surface areas of FeS were measured by using an X-Ray Fluorescence (XRF, EAGLE III, USA) and a Brunauer-Emmett-Teller (BET, BK112T-B, Micromeritics, USA), respectively. The crystal structure of FeS was characterized by a XRD (MAXima-X-7000, Shimadzu, Japan) with Cu Kα radiation over the 2θ range of 5-85^0. The XPS spectra of FeS material in this study were analyzed by using a X-ray photoelectron spectroscopy (XPS, AXIS-Ultradld-600WX, Shimadzu Japan).

Text S4. Calculation of Fukui index for CBZ

Fukui function based on the density functional theory (DFT) was used to predict the regioselectivity of reactive radicals towards the CBZ molecules. All of the calculations were performed using the Materials Studio DMol3 software package from Accelrys (version 2019). Fukui function is an important concept in the conceptual density functional theory (CDFT), and it has been widely used in prediction of reactive sites of electrophilic and nucleophilic attacks [3-5].

The condensed Fukui function (*f*) can be calculated as:

Electrophilic attack: $f_A^- = q_{N-1}^A - q_N^A$ (S1)

Nucleophilic attack: $f_A^+ = q_N^A - q_{N+1}^A$ (S2)

Radical attack: $f^0 = (f_A^- + f_A^+)/2$ (S3)

where q^A is the atom charge of atom A at the corresponding state. The reactive sites on a molecule usually have larger values of Fukui index than other regions. •OH and $•SO_4^-$ have been classified as a kind of electrophile, which are more likely to attack the sites that can readily lose electrons [2]. Thus, we calculated the Fukui index (f^+, f^-, and f^0) of CBZ for electrophilic and radical attacks.

Text S5. Kinetic analysis of experimental data

To explore the degradation mechanism, using an FeS dosing of 125 mg/L as an example, the kinetic data were fitted by three commonly used models (pseudo zero-order, pseudo-1st-order, and 2nd-order, and these kinetic parameters, along with the correlation coefficient (R^2), were also reported in Table S2.

As can be seen from Table S2, the pseudo-1st-order model (R^2=0.9937) was found to match the data slightly better than the other two models proposed (R^2=0.9268 and R^2=0.8158). Consequently, it was concluded that the CBZ oxidation reaction was more in line with the pseudo 1-st reaction kinetics, the experimental data were mainly fitted by the pseudo 1st order model in the following studies.

The fitting results for different dosages of FeS and $S_2O_8^{2-}$, and different initial pH conditions are shown in Table S3-S5, respectively.

B. Supplementary Tables

Table S1 Physicochemical properties of CBZ

Parameters	value	Parameters	value
Chemical formula	$C_{15}H_{12}N_2O$	Density	1.266 g/cm^3
Molecular Weight	236.27 g/mol	pKa	pK_{a1}=1, pK_{a2}=13.9;
Melting point	189~192 ºC	Solubility in water	17.7 mg/L (25℃)
Chemical structure	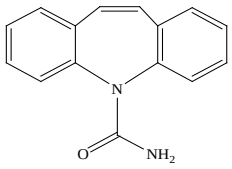	$logK_{ow}$	2.25

Table S2 Fitted parameters for CBZ degradation by FeS-$S_2O_8^{2-}$ with three models

Models	Equations	Kinetic equations	R^2
0 order	$\frac{dC}{dt} = k$	$C(CBZ_t)/C(CBZ_0)$= -0.0162t + 0.8908	0.9268
1st-order	$\frac{dC}{dt} = kC$	$Ln(C(CBZ_t)/C(CBZ_0))$= -0.0520t + 0.1166	0.9937
2nd-order	$\frac{dC}{dt} = kC_1C_2$	$C(CBZ_0)$ /$C(CBZ_t)$ = 0.3175t – 1.6979	0.8158

Note: k was the degradation rate constant, C_1 and C_2 were the concentrations of two reactants, respectively;

Table S3 The fitting results for different dosages of FeS by pseudo-first-order model

FeS dosage (mg/L)	Kinetic equations	k_{obs} (min^{-1})	R^2
50	$Ln(C(CBZ_t)/C(CBZ_0))=-0.0172t - 0.0219$	0.0172	0.9950
125	$Ln(C(CBZ_t)/C(CBZ_0))=-0.0520t + 0.1166$	0.0520	0.9937
250	$Ln(C(CBZ_t)/C(CBZ_0))=-0.1225t + 0.0532$	0.1225	0.9936
500	$Ln(C(CBZ_t)/C(CBZ_0))=-0.1573t - 0.1176$	0.1573	0.9726

Table S4 The fitting results for different dosages of $S_2O_8^{2-}$ by pseudo-first-order model

Initial contents of $S_2O_8^{2-}$ (mM)	kinetic equations	k_{obs} (min^{-1})	R^2
0.1	$Ln(C(CBZ_t)/C(CBZ_0))= -0.0111t - 0.0042$	0.0111	0.9947
0.3	$Ln(C(CBZ_t)/C(CBZ_0))= -0.0586t + 0.1173$	0.0586	0.9927
0.5	$Ln(C(CBZ_t)/C(CBZ_0))= -0.1225t + 0.0532$	0.1225	0.9936
1.0	$Ln(C(CBZ_t)/C(CBZ_0))= -0.1588t - 0.1470$	0.1588	0.9534

Table S5 The fitting results for various initial pH by pseudo-first-order model

Initial pH	kinetic equations	k_{obs} (min^{-1})	R^2
3.0	$Ln(C(CBZ_t)/C(CBZ_0))= -0.1751t - 0.4649$	0.1751	0.9377
6.0	$Ln(C(CBZ_t)/C(CBZ_0))= -0.1225t + 0.0532$	0.1225	0.9936
7.0	$Ln(C(CBZ_t)/C(CBZ_0))= -0.0795t + 0.2793$	0.0795	0.9866
9.0	$Ln(C(CBZ_t)/C(CBZ_0))= -0.0034t - 0.0445$	0.0034	0.9009

C. Supplementary Figures

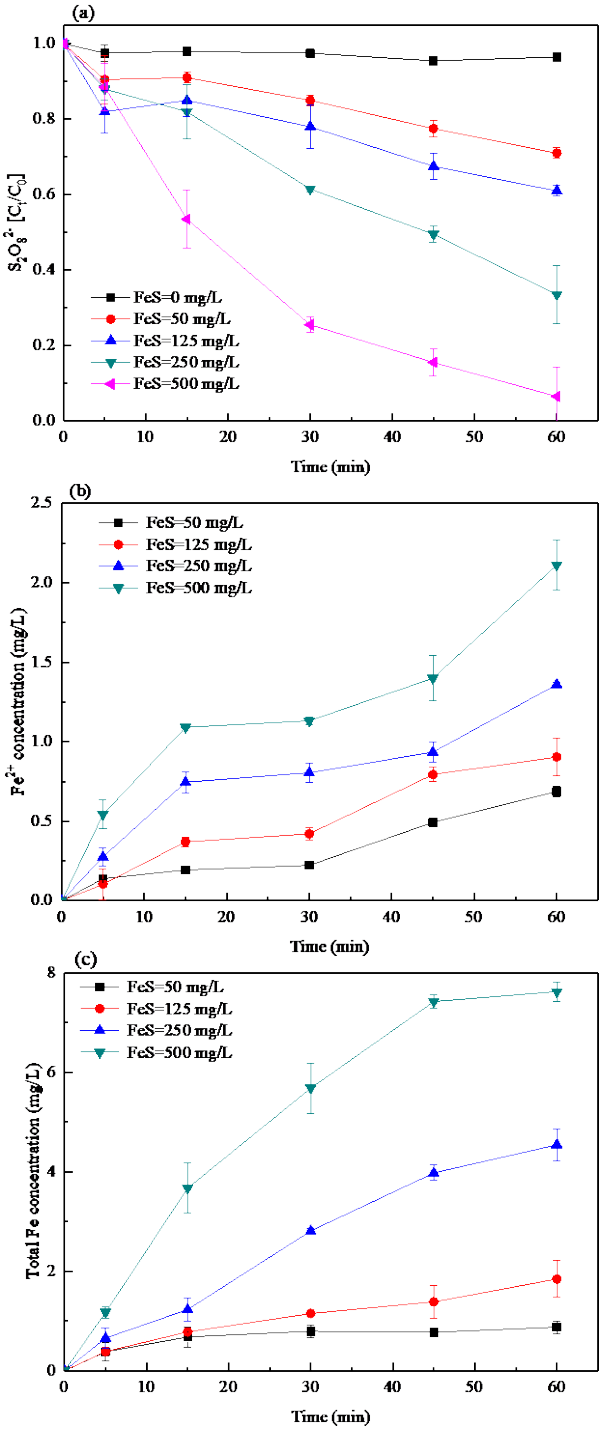

Fig. S1 Effects of different FeS dosages on the decomposition of $S_2O_8^{2-}$ (a), and the evolutions of Fe^{2+} (b), and total Fe (c) in solution; ([CBZ]$_0$=10 mg/L, [$S_2O_8^{2-}$]=0.5 mM, initial pH=6.0, T=25^{0}C)

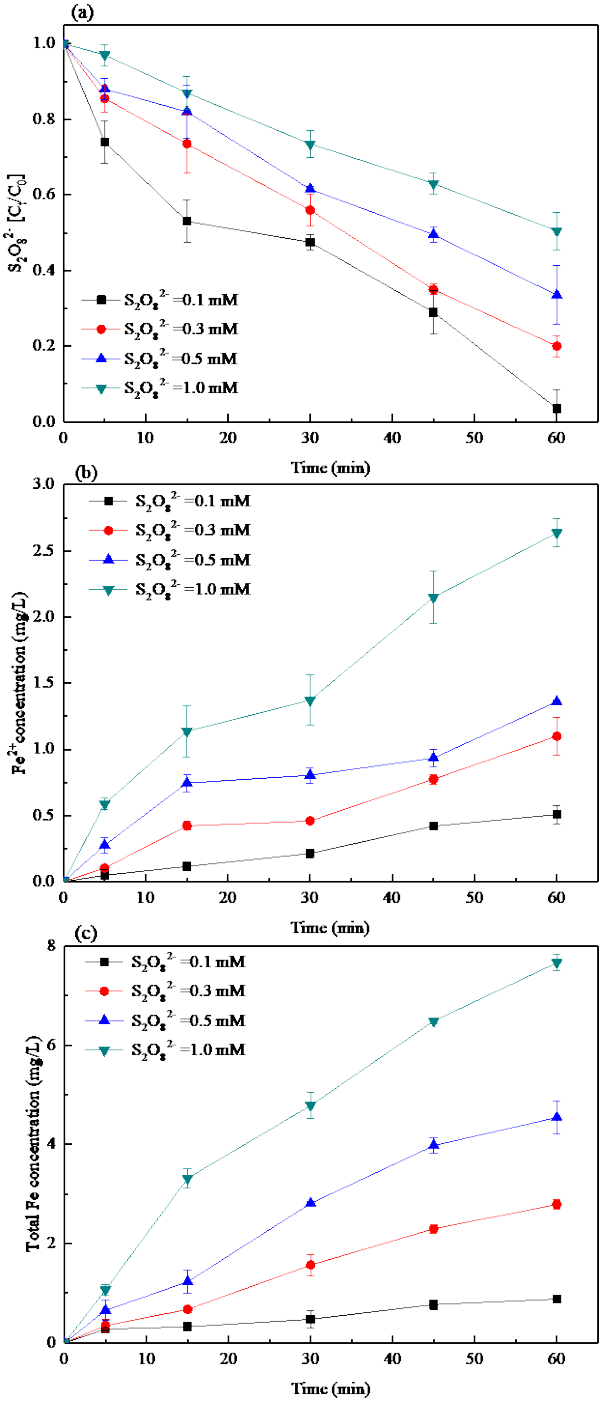

Fig. S2 Effects of different initial $S_2O_8^{2-}$ concentrations on the decomposition of $S_2O_8^{2-}$ (a), the evolutions of Fe^{2+} (b), and total Fe (c) in solution; ($[CBZ]_0$=10mg/L, [FeS]=250mg/L, initial pH=6.0, T=25^{0}C)

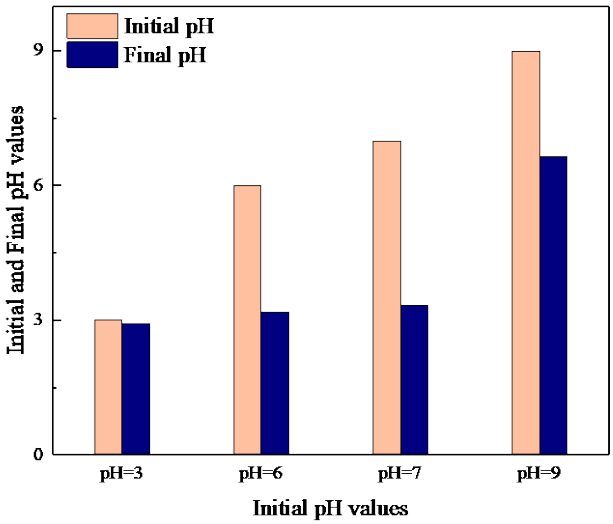

Fig. S3 The final pH values under the different initial pH conditions in the FeS-$S_2O_8^{2-}$ process; ($[CBZ]_0$=10mg/L, [FeS]=250mg/L, $[S_2O_8^{2-}]$=0.5mM, T=25^0C)

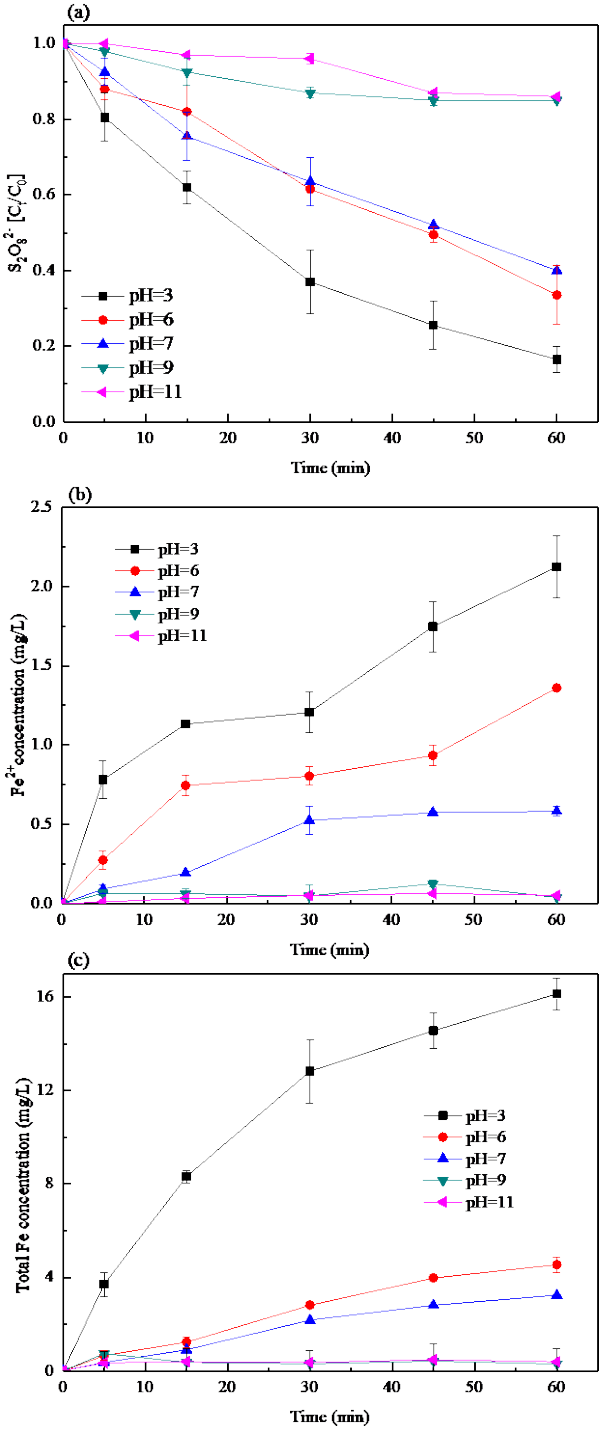

Fig. S4 Effects of different initial pH values on the decomposition of $S_2O_8^{2-}$ (a), the evolutions of Fe^{2+} (b), and total Fe (c) in solution in the FeS-$S_2O_8^{2-}$ process; ([CBZ]$_0$=10mg/L, [FeS]=250mg/L, [$S_2O_8^{2-}$]=0.5mM, T=25^{0}C)

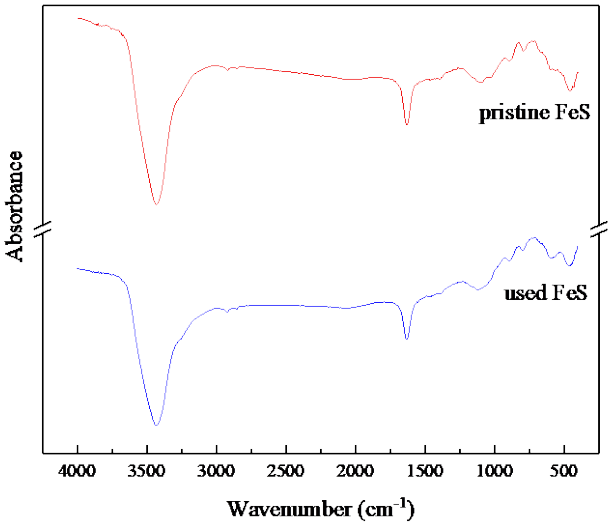

Fig. S5 FTIR spectrum of the FeS before and after reaction

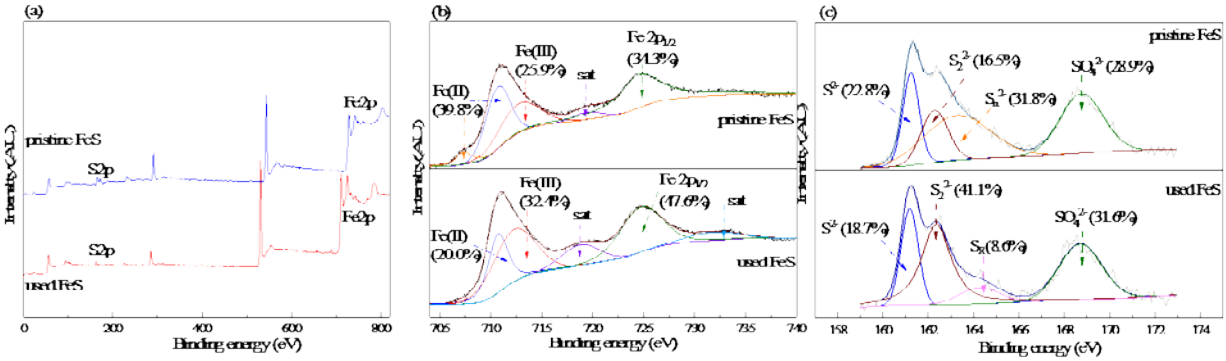

Fig. S6 XPS survey of FeS before and after CBZ degradation (a), high resolution XPS spectra of Fe 2p (b) and S 2p (c) for the samples before and after CBZ degradation

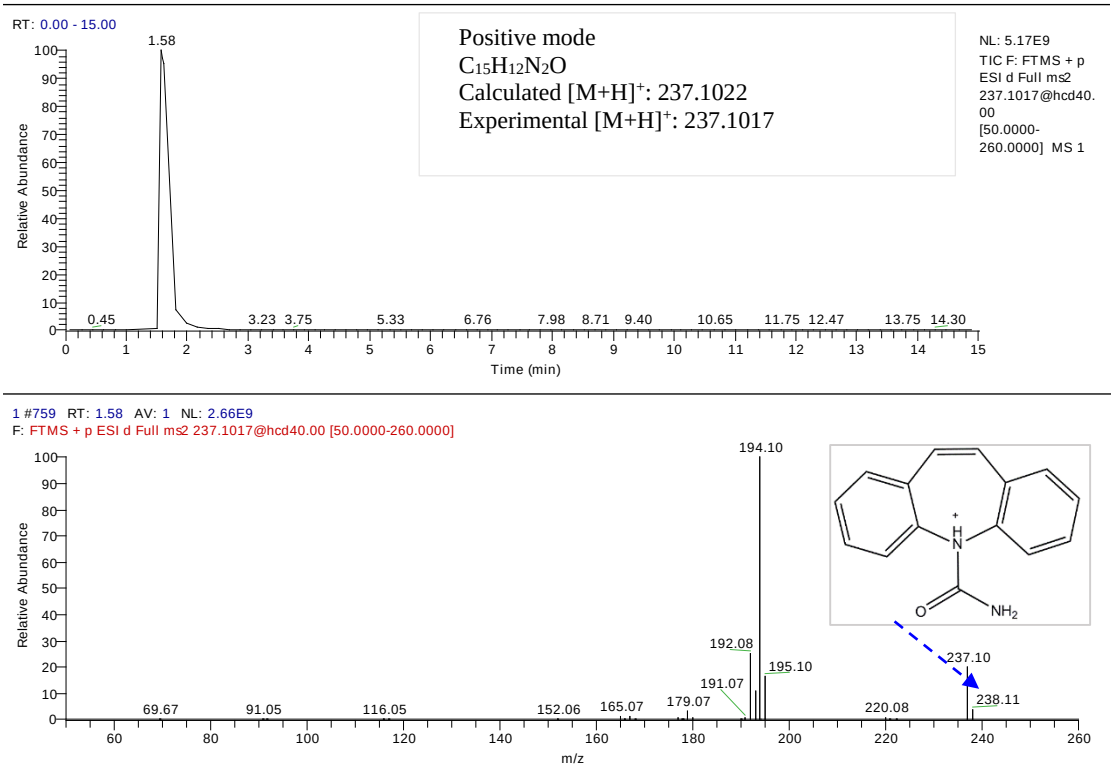

Fig. S7 Identification of CBZ ([M+H]$^+$=237)

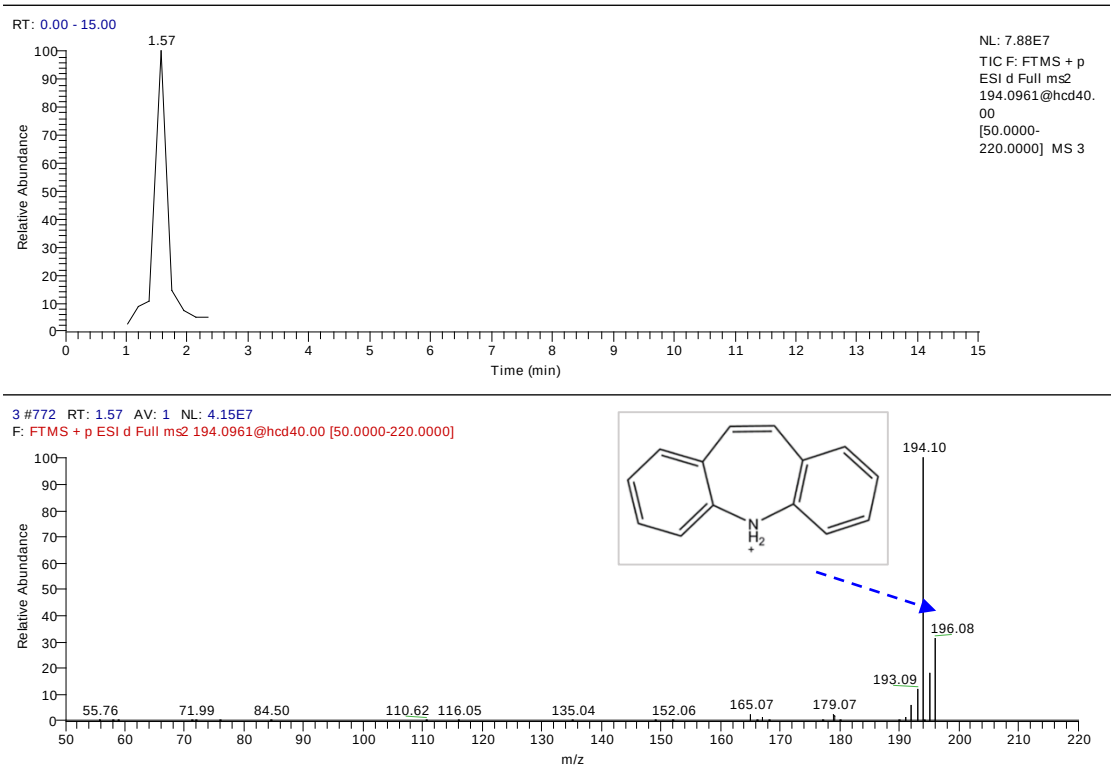

Fig. S8 Identification of IM-9 ([M+H]$^+$=194)

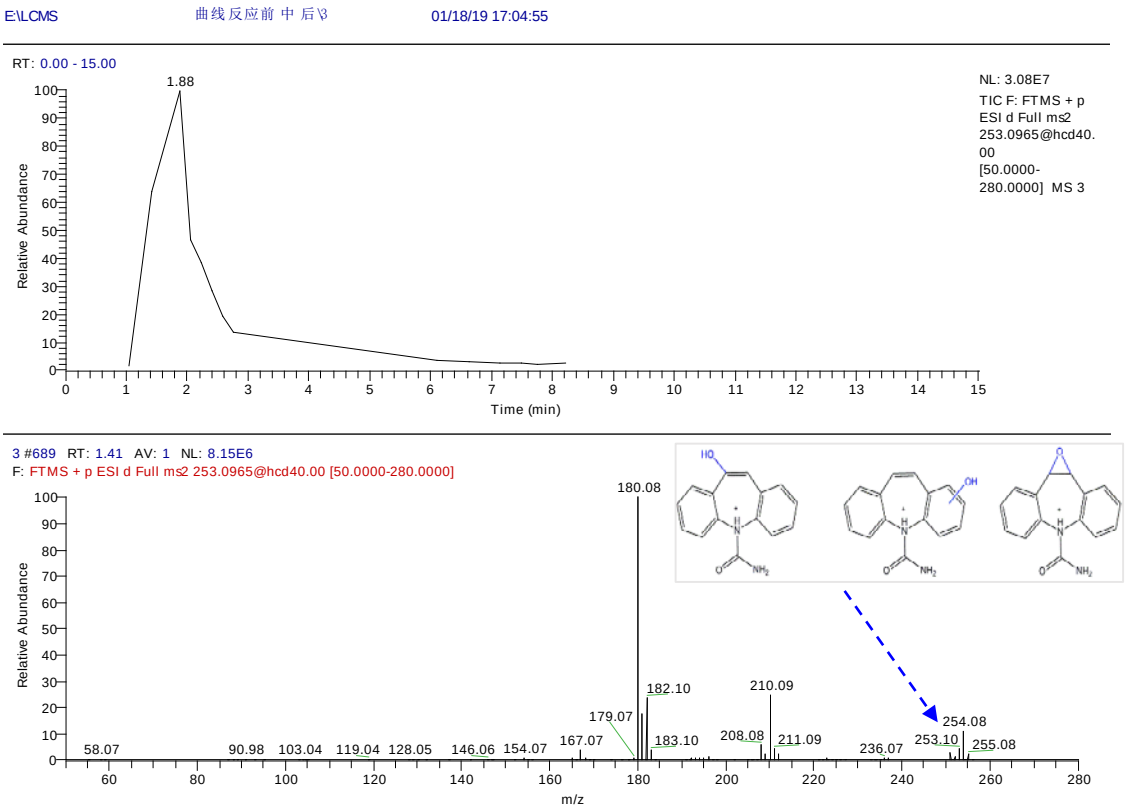

Fig. S9 Identification of IM-1-5 ($[M+H]^+$=253)

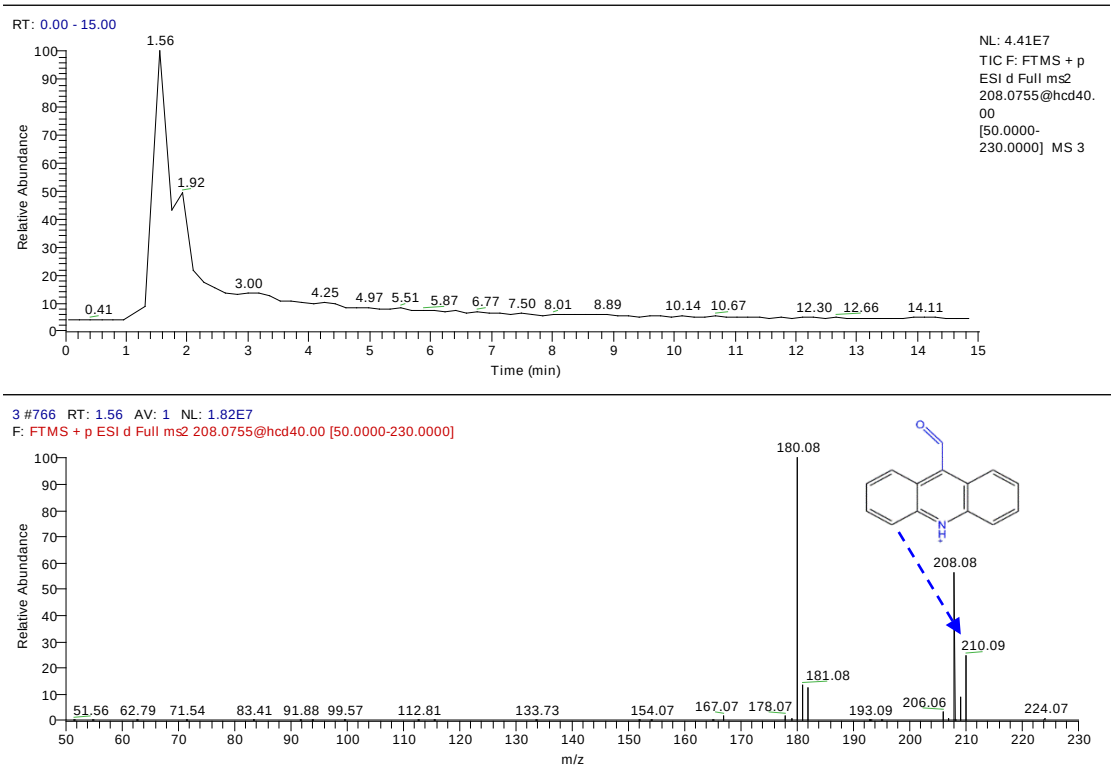

Fig. S10 Identification of IM-6 ([M+H]$^+$=208)

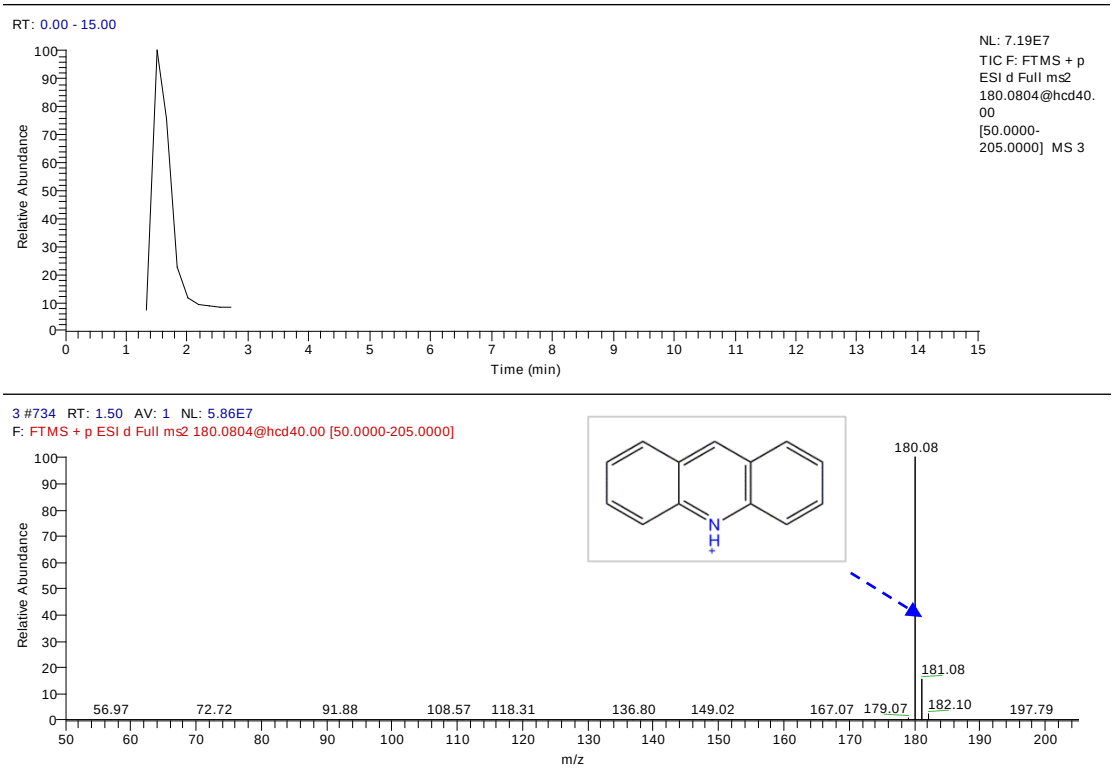

Fig. S11 Identification of IM-7 ([M+H]$^+$=180)

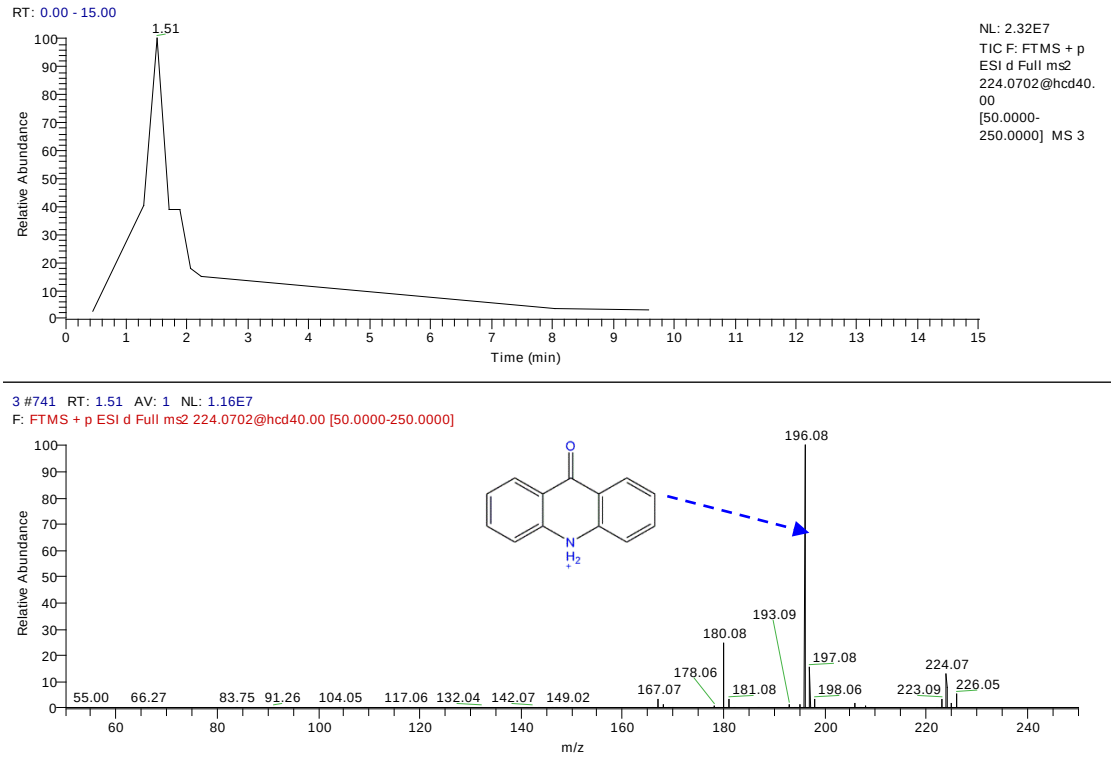

Fig. S12 Identification of IM-8 ([M+H]$^+$=196)

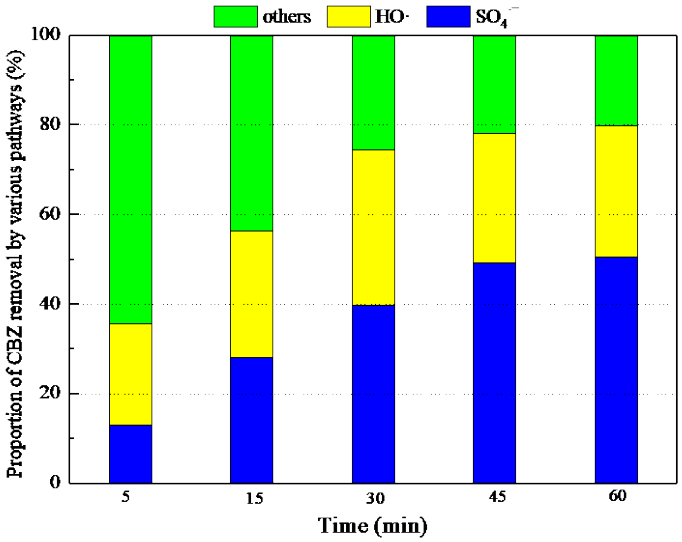

Fig. S13 The relative contribution of CBZ degradation by three pathways at different time in the FeS-$S_2O_8^{2-}$ process; ($[CBZ]_0$=10mg/L, [FeS]=250mg/L, $[S_2O_8^{2-}]$=0.5mM, T=25^0C);

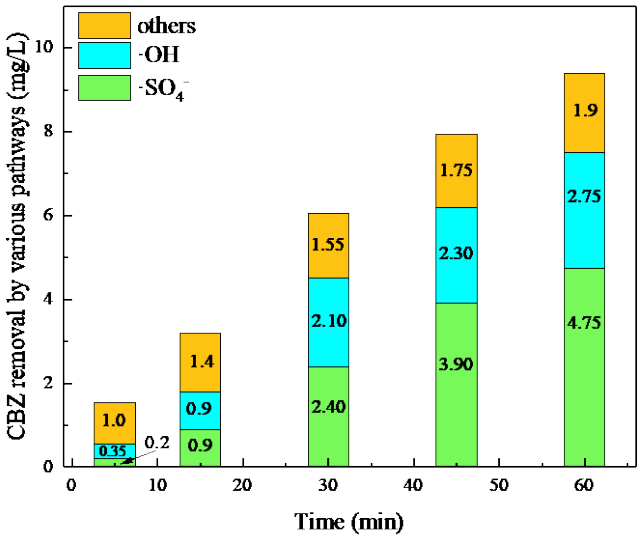

Fig. S14 The degradation amount of CBZ by various pathways in the FeS-$S_2O_8^{2-}$ process; ($[CBZ]_0$=10mg/L, [FeS]=250mg/L, $[S_2O_8^{2-}]$=0.5mM, T=25^0C);

D. Reference

[1] Huang, M., Zhou, T, Wu, X., Mao, J. Distinguishing homogeneous heterogeneous degradation of norfloxacin in a photochemical Fenton-like system (Fe3O4/UV/oxalate) and the interfacial reaction mechanism, Water Res. 119, (2017) 47–56.

[2] De Vleeschouwer, F., Van Speybroeck, V., Waroquier, M., Geerlings, P. and De Proft, F. (2007) Electrophilicity and nucleophilicity index for radicals. Org. Lett. 9(14), 2721-2724.

[3] Parr, R.G. and Yang, W.T. (1984) Density functional-approach to the frontier-electron theory of chemical-reactivity. J. Am. Chem. Soc. 106(14), 4049-4050.

[4] Pan, F., Ji, H., Du, P., Huang, T., Wang, C., Liu, W., 2021. Insights into catalytic activation of peroxymonosulfate for carbamazepine degradation by MnO2 nanoparticles in-situ anchored titanate nanotubes: Mechanism, ecotoxicity and DFT study. Journal of hazardous materials 402, 123779.

[5] Chen, H., Zhang. Z., Feng, M., Liu,W., Wang, W., Yang, Q., Hu, Y. Degradation of 2,4-dichlorophenoxyacetic acid in water by persulfate activated with FeS (mackinawite), Chem. Eng. J. 313 (2017) 498–507.